Journal of Photochemistry and Photobiology A: Chemistry 209 (2010) 174–180

Contents lists available at ScienceDirect

Journal of Photochemistry and Photobiology A: Chemistry

journal homepage: www.elsevier.com/locate/jphotochem

Influence of amylopectin in dimethylsulfoxide on the improved performance of dye-sensitized solar cells

Young-Sam Jung[a], A.R. Sathiya Priya[a], Min Ki Lim[b], Seung Yong Lee[b], Kang-Jin Kim[a,*]

[a] Department of Chemistry, Korea University, 5 Ka, Anam Dong, Seoul 136-713, Republic of Korea
[b] DongWoo Fine-Chem, Iksan-si, Jeonbuk 802-8, Republic of Korea

ARTICLE INFO

Article history:
Received 11 July 2009
Received in revised form
24 September 2009
Accepted 16 November 2009
Available online 20 November 2009

Keywords:
Amylopectin–I_2 complex
Long-term stability
Dye-sensitized solar cell
Short-circuit photocurrent
Corrosion resistant
Open-circuit voltage

ABSTRACT

A highly viscous liquid electrolyte is prepared by adding a small amount of amylopectin into dimethylsulfoxide solvent. By using this viscous electrolyte, a dye-sensitized solar cell (DSSC) enhances the short-circuit photocurrent density and solar-to-electricity conversion efficiency by 22% and 8.4%, respectively, compared to those obtained with the reference cell without amylopectin. Furthermore, the stability of the DSSC is enormously improved by the addition of amylopectin. Polarization curves indicate that amylopectin is a reasonable corrosion inhibitor for silver metal in the electrolyte containing I_3^-/I^- couple.

1. Introduction

Interest in the development of new types of solar cells has been spurred by public concern about pollution and energy consumption. The principle of operation of the dye-sensitized solar cell (DSSC) involves the photoexcitation of the sensitizer, followed by electron injection into the conduction band of the semiconductor oxide film. The dye molecule is regenerated by the redox system, which is itself regenerated at the counter electrode by the electrons that have passed through the load. The redox electrolyte constitutes the internal conducting channel and conduction occurs through the diffusion of the charge carriers, I_3^- and I^-, between the TiO_2 film and the platinized counter electrode [1].

Solid polymer electrolytes (SPE) have been extensively studied in the last two decades because of their potential in many technological areas, including solid-state batteries, chemical sensors and electrochromic devices [2–4]. Polymer electrolytes obtained from natural polymers, such as starch and cellulose derivatives like hydroxyethylcellulose and hydroxypropylcellulose, have attracted attention in recent times, because of their superior mechanical and electrical properties [5–9]. Both starch and cellulose are abundant, renewable, and biodegradable natural polymers and their use offers a promising alternative for the development of new SPE materials.

The major component of starch from sources like potatoes and corn is amylopectin with amylose being a minor component. While the blue complex of iodine with amylose is well known and has been extensively studied, the red complex of iodine with amylopectin is less well known and very little attention has been given to its characterization. It was recently identified that four iodine atoms are more or less linearly arranged within the cavity of the helix structure of 11 anhydroglucose residues to form the chromophore group in the amylopectin–iodine complex, as schematically shown in Fig. 1 [10].

Currently, state-of-the-art DSSCs have an overall light conversion efficiency greater than 11% under an irradiation level of 100 mW cm^{-2} (AM 1.5) [11,12]. However, the potential problems caused by liquid electrolytes, such as the leakage and volatilization of the liquid, possible desorption and photodegradation of the anchored dyes, and the corrosion of the Pt counter electrode by iodine in the electrolytic solution, have had the effect of limiting the long-term performance and practical use of these DSSCs. In order to increase the long-term stability of DSSCs, many attempts have been made to replace the liquid electrolytes with p-type semiconductors [13,14], organic hole transport materials [15–17], or polymer gel electrolytes [18–27]. Although the use of solid-state electrolytes solves some of these problems, they show a lower energy conversion efficiency than liquid electrolytes because of the poor contact

* Corresponding author. Tel.: +82 2 3290 3127; fax: +82 2 3290 3121.
E-mail address: kjkim@korea.ac.kr (K.-J. Kim).

1010-6030/$ – see front matter © 2009 Elsevier B.V. All rights reserved.
doi:10.1016/j.jphotochem.2009.11.011

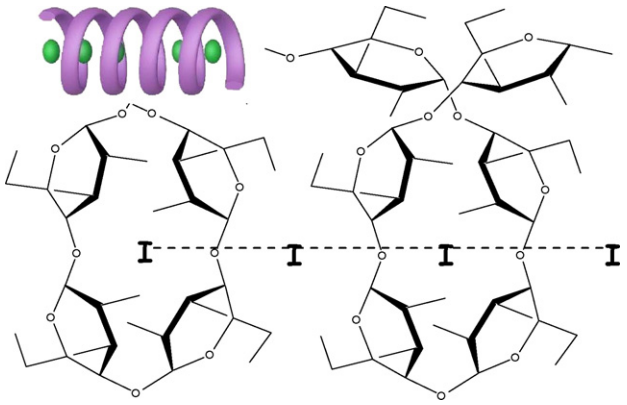

Fig. 1. Schematic representation of amylopectin–I_2 complex. Inset shows its three dimensional structure.

of the solid-state charge transport material with the dye-coated TiO_2 surface. Polymer gel electrolytes have some advantages, such as a low vapor pressure, good long-term stability, excellent contacting and filling properties between the nanostructured working electrode and counter electrode, and higher ionic conductivity.

In particular, scaling up of the DSSC from laboratory scale to practical applications requires silver grid as current collector to reduce sheet resistance of the conducting glass substrate. However, silver grid should be protected to reduce its corrosion by iodine in the electrolytic solution and to decrease the dark current via charge recombination. The protection of silver grid from I_2 has been studied by Surlyn sheet lamination or glass frit layer [28].

In the present study using amylopectin as the polymer host for the first time, dimethylsulfoxide (DMSO) as an organic solvent, and lithium iodide and iodine as the source of I_3^-/I^-, an electrolyte with high viscosity was prepared. Amylopectin was found to be practically insoluble in all commonly utilized organic solvents except DMSO. The influence of amylopectin on the corrosion of silver metal and long-term stability and performance of the DSSCs is investigated and compared with those of the cells containing conventional liquid electrolytes.

2. Experimental

Viscosity measurements were conducted under an Ar atmosphere using an SV-10 viscometer. Cyclic voltammograms were obtained in the electrolyte solution containing 1 mM I_2, 10 mM LiI and 0.1 M $LiClO_4$ in DMSO with and without 1.5×10^{-2} M amylopectin at a scan rate of 100 mV s^{-1} using an EG&G PARC 263A potentiostat. The electrochemical cell consisted of a Pt working electrode (1.6 mm diameter, MF-2013, Bioanalytical Systems, Inc.), a Pt-wire auxiliary electrode and an Ag/AgCl reference electrode. Chronoamperometric curves were also obtained from the DMSO solutions containing 0.6 M 1-hexyl-2,3-dimethylimidazolium iodide, 0.05 M I_2, 0.1 M LiI, and 0.5 M 4-*tert*-butylpyridine with and without 1.5×10^{-2} M amylopectin using an EG&G PARC 263A potentiostat, with an electrochemical cell consisting of a Pt microelectrode (MF-2013), a Pt-wire auxiliary electrode and an Ag/AgCl reference electrode. The potentials were applied at 1.00 V and −1.00 V for the oxidation of I^- and reduction of I_3^-, respectively. Amylopectin hydrate (A0456, TCI) derived from waxy corn was used.

Dye-coated TiO_2 films were prepared as the working electrodes for the DSSCs as follows [29]. In each case, a thin buffer layer of non-porous TiO_2 was deposited on a cleaned FTO conducting glass, purchased from Libbey-Owens-Ford (TEC 8, 75% transmittance in the visible region), from 5% titanium(IV) butoxide in ethanol by spin coating at 3000 rpm. The thin layer coated FTO glass was cleaned and annealed at 450 °C. Dyesol titania paste, purchased from Dyesol Ltd., was deposited on the above-pretreated FTO glass by the doctor blade technique, using 2 scotch tapes to limit the thickness of the film. The film was dried for 10 min at 70 °C, followed by removing the tape and coating the film with 2% $TiCl_4$ solution by the spin coating method and annealing it at 450 °C for 30 min. A porous TiO_2 film consisting of anatase crystalline size of approximately 20 nm with a thickness of about 10 μm was thus produced. The annealed film was sensitized with N719 dye by immersing it for 24 h in an ethanol solution of N719 dye (0.3 mM of $(Ru(II)L_2(NCS)_2)$:2TBA, where L = 2,2′-bipyridyl-4,4′-dicarboxylic acid, Solaronix SA). A 2-electrode sandwiched DSSC was fabricated according to the procedure described elsewhere [29]. The DSSC had an active area of 0.4 cm × 0.4 cm. The electrolyte consisted of 0.05 M I_2, 0.1 M LiI, 0.6 M 1,2-dimethyl-3-hexylimidazolium iodide, and 0.5 M 4-*tert*-butylpyridine in DMSO with amylopectin. The two small holes used for introducing electrolyte in the counter electrode were sealed with small squares of Kapton polyimide film (DuPont) with a silicon adhesive instead of using microscope objective glass. This was to amplify the difference of the decreases in photocurrent and efficiency between with and without amylopectin. Reference DSSCs were also prepared under identical conditions without amylopectin.

The photocurrent density–voltage (*J*–*V*) curves of the DSSCs fabricated with and without amylopectin were obtained using a Keithley M236 source measure unit. A 300 W Xe arc lamp (Oriel) with an AM 1.5 solar simulating filter for spectral correction served as the light source, and its light intensity was adjusted to 100 mW cm^{-2} by using a Si solar cell. Thermally sealed cells were used to test the long-term stability of the solar cells. The sealed cells were stored in a desiccator and subjected to electrochemical measurements every 24 h in order to study their long-term stability. To complement the photocurrent behavior of the DSSCs, electrochemical impedance spectra were recorded using an EG&G PARC 273A potentiostat with a M1025 frequency-response detector. The cell consisted of two Pt-coated FTO electrodes with an area of 1 cm^2 under the dark condition over a frequency range of 0.05–10^5 Hz with an AC amplitude of 5 mV. The data were analyzed using ZView (Scribner Associates, Inc.) software. The incident photon-to-current conversion efficiency (IPCE) of the DSSCs was measured using a photon counting spectrofluorometer (ISS PC1), equipped with a 350 W Xe lamp and a motorized monochromator. Tafel plots for the corrosion of silver were obtained with an EG&G PARC 273A potentiostat at a scan rate of 100 mV s^{-1}, using an electrochemical cell consisting of a printed Ag-film working electrode (5 mm × 5 mm on glass), a Pt-wire auxiliary electrode and a Pt-wire reference electrode.

3. Results and discussion

3.1. Characterizations of the electrolyte

The determination of the viscosity is essential to obtain a complete understanding of the influence of amylopectin. Moreover, the viscosity data yield important information on the possible later application of the electrolyte mixture in electrochemical devices. The recorded viscosities of the electrolyte containing 0.6 M 1,2-dimethyl-3-hexylimidazolium iodide, 0.1 M LiI, 0.05 M I_2, and 0.5 M 4-*tert*-butylpyridine in DMSO are given in Table 1. The viscosity of the electrolyte increased enormously from 2.07 mPa s to 73.67 mPa s with the addition of 1.5×10^{-2} M amylopectin. Amylopectin was found to be soluble in DMSO, but practically insoluble in 3-methoxypropionitrile, acetonitrile, tetrahydrofuran, formamide, *N*,*N*′-dimethylformamide, *N*-methylformamide, and *N*-methylpyrrolidone, which are the solvents that are commonly utilized in DSSCs [30].

Table 1
Viscosity of the electrolyte with and without 1.5×10^{-2} M amylopectin.

Electrolyte[a]	Viscosity (mPa s)
Without	2.1
With	73.7

[a] Electrolyte consisted of 0.6 M 1,2-dimethyl-3-hexylimidazolium iodide, 0.1 M LiI, 0.05 M I_2, and 0.5 M 4-*tert*-butylpyridine in DMSO.

3.2. Photovoltaic performance

In order to investigate the photoelectrochemical properties of the DSSCs with electrolytes based on amylopectin, a series of cells with different concentrations of amylopectin were fabricated using the electrolytes consisting 0.05 M I_2, 0.1 M LiI, 0.5 M 4-*tert*-butylpyridine, and 0.6 M 1,2-dimethyl-3-hexylimidazolium iodide in DMSO. The resulting photocurrent density–voltage (J–V) curves are shown in Fig. 2 and Table 2 lists the measured photoelectrochemical data of the above cells. The J–V curves for 2.2×10^{-3} M and 1.5×10^{-2} M amylopectin were also measured but not included in the figure for clarity. These data reveal that the photoelectrochemical performance of the cells was dependent on the amylopectin concentration in the electrolytes. The cell with 1.5×10^{-2} M amylopectin yielded a short-circuit current density (J_{sc}) of 6.83 mA cm^{-2}, an open-circuit voltage (V_{oc}) of 0.74 V, an overall solar-to-electricity conversion efficiency (η) of 3.34%, and a fill factor (FF) of 0.66. The reference cell without amylopectin yielded a J_{sc} of 5.58 mA cm^{-2}, V_{oc} of 0.80 V, η of 3.08%, and FF of 0.69. The J_{sc} and η were found low due to the use of DMSO as solvent. Recently, the efficiency of only 1.37% has been reported for the DSSC using N3 dye in the DMSO solution containing 1-methyl-3-propylimidazolium iodide [31]. Nevertheless, it is noted that the η increased by 8.4% with the inclusion of 1.5×10^{-2} M amylopectin compared to the case in the absence of amylopectin, which is mostly attributed to the large increase in J_{sc} by 22%.

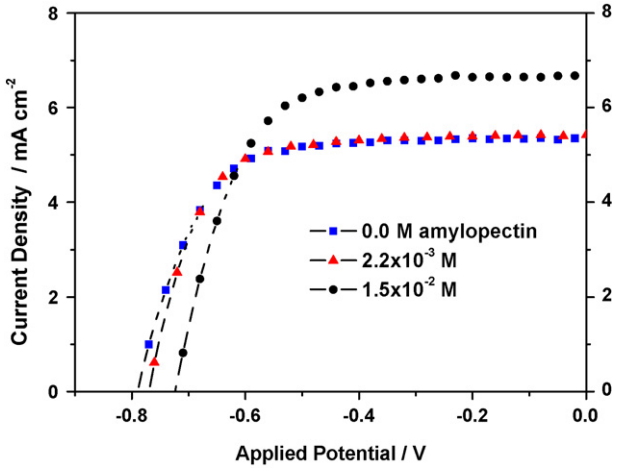

Fig. 2. Photocurrent–voltage curves of the DSSCs *vs.* concentration of amylopectin. The light intensity was 100 mW cm^{-2}.

Table 2
Photovoltaic parameters of the DSSCs fabricated using different electrolytes[a].

Amylopectin (M)	J_{sc} (mA cm^{-2})	V_{oc} (V)	FF	η (%)
0.0	5.58	0.80	0.69	3.08
2.2×10^{-3}	5.41	0.77	0.71	2.96
8.7×10^{-3}	5.57	0.76	0.70	2.96
1.5×10^{-2}	6.83	0.74	0.66	3.34
2.2×10^{-2}	6.74	0.73	0.67	3.30

[a] The same electrolyte as in Table 1.

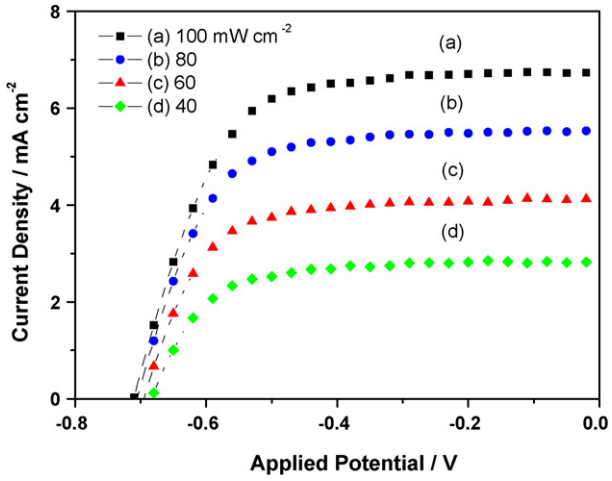

Fig. 3. Photocurrent–voltage curves of the DSSCs with 1.5×10^{-2} M of amylopectin at various light intensities.

The J–V curves as a function of the incident light intensity for the DSSC employing an amylopectin-containing electrolyte are shown in Fig. 3. These curves were measured at light intensities of 40 mW cm^{-2}, 60 mW cm^{-2}, 80 mW cm^{-2} and 100 mW cm^{-2}. Despite the enormous increase in the viscosity of the electrolyte in the presence of amylopectin, a linear photocurrent response to the solar light intensity was observed. This result indicates that the electron diffusion in the TiO_2 film of the highly viscous electrolyte toward the back conducting contact is not limited by the presence of amylopectin in the film up to a light intensity of 100 mW cm^{-2}.

3.3. J_{sc} increase

The J_{sc} increases with the additive when it is present above 8.7×10^{-3} M (Table 2). This is confirmed by the incident photon-to-current conversion efficiency (IPCE) of the DSSCs as shown in Fig. 4. The increase in the J_{sc} value was attributed to the structural change of the electrolyte associated with the formation of the amylopectin–I_2 complex shown in Fig. 1 [10], which is advantageous for the performance of the DSSC. Amylopectin contains numerous amylose-like chains of up to 30 glucose residues linked through alpha (1–4) bonds, connected to one another through alpha

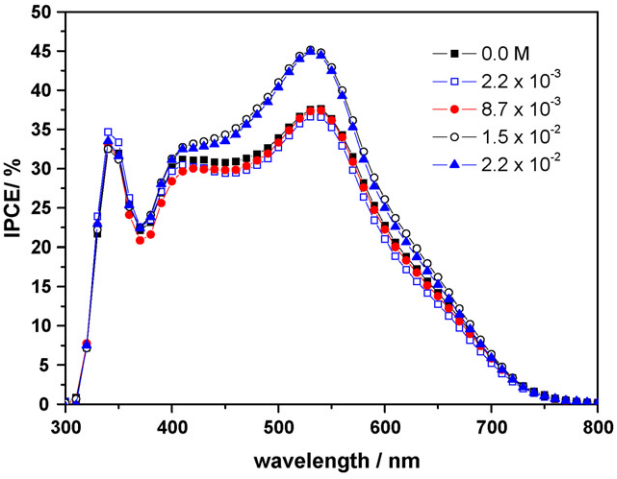

Fig. 4. IPCE spectra of the DSSCs assembled with the electrolytes containing different concentrations of amylopectin.

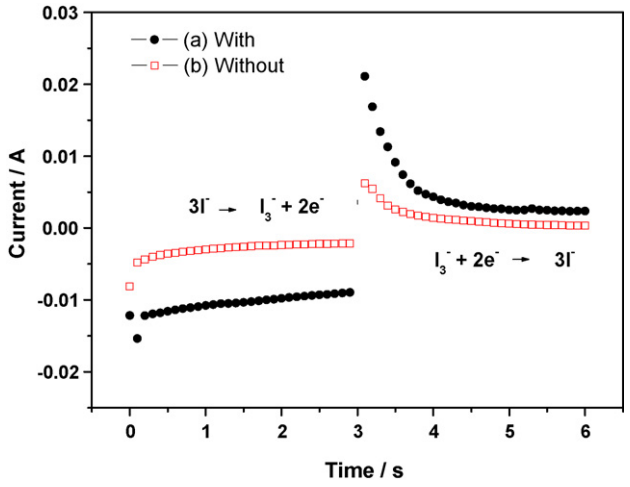

Fig. 5. Chronoamperometric curves in the electrolyte (a) with and (b) without 1.5×10^{-2} M amylopectin in DMSO.

(1–6) branch points. That is, this three-dimensional arrangement seems to form efficient ion transport channels and thus facilitates the ionic transport of the charge carriers through the electrolyte, thereby leading to the enhancement of the photocurrent compared to that in the reference electrolyte. However, at the low concentrations of amylopectin at 2.2×10^{-3} M and 8.7×10^{-3} M, the increased viscosity seems to play more dominant roles than the formation of the ion transport channels, resulting in the decreased J_{sc} values.

The enhancement of the ionic transport afforded by amylopectin above was supported by the chronoamperometric plots shown in Fig. 5. Each plot was obtained in DMSO solution using a Pt microelectrode, Pt-wire auxiliary electrode and Ag/AgCl reference electrode. The electrolyte with amylopectin consistently showed larger currents for both I_3^- reduction and I^- oxidation than the one without amylopectin. The enhancement of the current indicates that the diffusion coefficients of I_3^- and I^- are increased by the addition of amylopectin to the reference electrolyte, despite the resulting enormous increase in the viscosity of the electrolyte. To support further the enhanced diffusion of the charge carriers due to the network structure of amylopectin, electrochemical impedance spectra were measured. Fig. 6 compares the Nyquist plots of the electrochemical cells which contained the electrolyte with and without amylopectin and consisted of two Pt-coated FTO

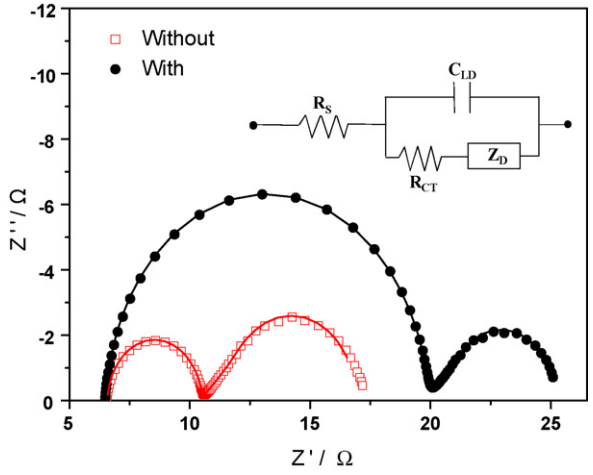

Fig. 6. Nyquist plots of the electrochemical cells containing different concentrations of amylopectin over a frequency range of 0.05–10^5 Hz with an AC amplitude of 5 mV.

Table 3
Electrochemical parameters obtained by fitting the EIS data of DSSCs assembled with and without 1.5×10^{-2} M amylopectin, using the equivalent circuit[a].

Electrolyte[b]	R_s (Ω cm^{-2})	R_{ct} (Ω cm^{-2})	C_{ld} (μF cm^{-2})	R_d (Ω cm^{-2})
Without	6.6	3.9	0.11	6.6
With	6.5	13.3	0.11	5.3

[a] Fitting of the spectra was performed with the ZView software.
[b] The same electrolyte as in Table 1.

electrodes. It is noted that TiO_2 and N719 were not included in the electrochemical cells. The corresponding electrochemical parameters were obtained by fitting the plots with the ZView software based on a standard Randles equivalent circuit [32]. The results listed in Table 3 show that the charge transfer resistance (R_{ct}) increases and the diffusion resistance (R_d) decreases while the series resistance (R_s) and Helmholtz capacitance (C_{dl}) remain the same with the addition of amylopectin. The decrease in the R_d is consistent with the chronoamperometric data above, confirming also that diffusion of charge carrier is enhanced in the presence of amylopectin. The increased R_{ct} may imply that the activation barrier for the electron transfer from the Pt electrode to I_3^- increases as a result of the amylopectin–I_2 complex formation.

3.4. V_{oc} decrease

Two possible reasons should be considered for the decrease in V_{oc} in the presence of amylopectin in DMSO: (i) the enhanced back electron transfer from the TiO_2 conduction band to the I_3^- ions in the electrolyte and (ii) the negative shift of the electrochemical potential of the I_3^-/I^- redox couple.

Firstly, the decrease in the V_{oc} value of the DSSC containing amylopectin by approximately 60 mV may be explained in terms of the enhanced rate of the back electron transfer from the TiO_2 conduction band to the I_3^- ions in the electrolyte (Eq. (1)). The V_{oc} value (Eq. (2)) kinetically manifests the rate of back electron transfer:

$$2e_{cb}^- + I_3^- \rightarrow 3I^- \quad (1)$$

$$V_{oc} = \left(\frac{kT}{e}\right) \ln\left(\frac{J_{sc}}{J_o}\right) \quad (2)$$

The J_o is the exchange current density and is related to the rate of the reaction (1):

$$J_o = k'[e_{cb}^-][I_3^-] \quad (3)$$

where k' is the rate constant involving the activation barrier for its reaction [33].

The increase in the J_{sc} value observed with amylopectin suggests that more I^- ions are converted to I_3^- ions in the TiO_2 film compared to the case without amylopectin, leading to an increase in the concentration of I_3^- ions. The increase in the concentration of I_3^- ions leads to the enhancement of the back electron-transfer rate. Consequently, the value of V_{oc} decreases, according to Eq. (2). In the case of the electrolyte with β-cyclodextrin, the increase in the concentration of I_3^- ions was apparently not observed [34]. However, the decrease in V_{oc} due to the increase in the I_3^- concentration may not be large possibly because the effective concentration of I_3^- is partially offset by the formation of amylopectin–I_2 complex [35].

Secondly, the possibility of there being a change in the reduction potential of the I_3^-/I^- couple (V_{red}) due to the formation of amylopectin–I_2 complex was investigated. Under Fermi level pinning, these two parameters are linked by Eq. (4) [36,37]:

$$V_{oc} = |V_{FB} - V_{red}| \quad (4)$$

where V_{FB} is the flatband potential of the dye-coated TiO_2 electrode. Assuming that the adsorption of amylopectin onto the TiO_2 film is

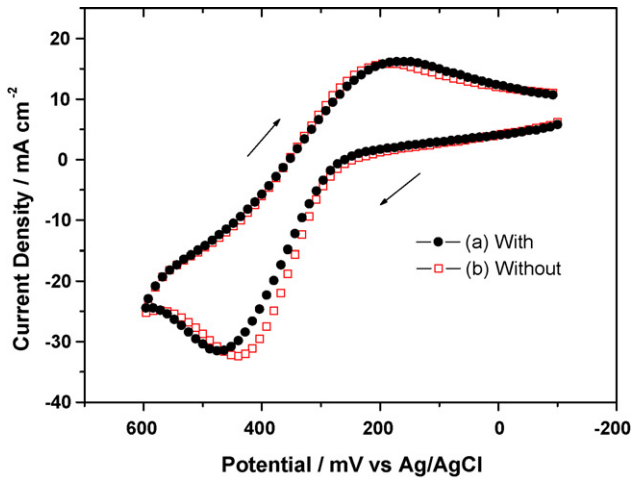

Fig. 7. Cyclic voltammograms obtained in the electrolyte containing 1 mM I_2, 10 mM LiI and 0.1 M $LiClO_4$ at a scan rate of 100 mV s^{-1} (a) with and (b) without 1.5×10^{-2} M amylopectin in DMSO.

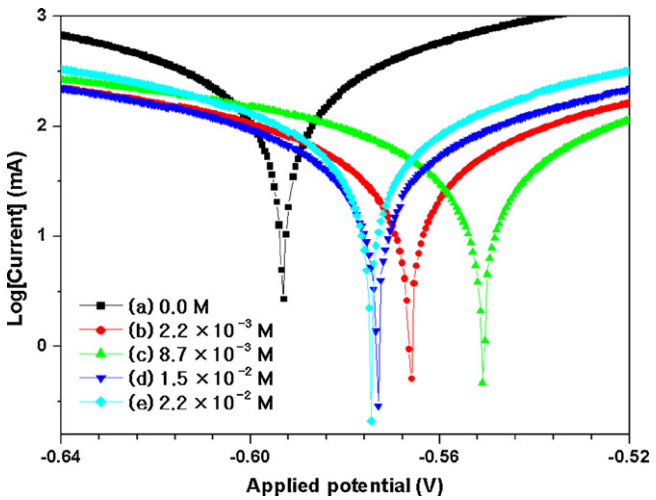

Fig. 8. Polarization curves for corroding of silver metal in the DMSO solutions with (a) 0.0 M, (b) 2.2×10^{-3} M, (c) 8.7×10^{-3} M, (d) 1.5×10^{-2} M, and (e) 2.2×10^{-2} M amylopectin.

not very significant, as evidenced by the same Helmholtz capacitance mentioned above, it is expected the V_{FB} remains the same, regardless of the absence or presence of amylopectin in the electrolyte. Under this condition, the decreased V_{oc} value of the DSSC containing amylopectin suggests that the V_{red} value of the I_3^-/I^- redox couple shifts negatively. To verify this notion, the change in the V_{red} value was examined by cyclic voltammetry. Fig. 7 shows the cyclic voltammograms (CVs) of the electrolyte with and without amylopectin. The CVs were obtained at a scan rate of 100 mV s^{-1}, using a cell assembled with a Pt working electrode, a Pt-wire auxiliary electrode and an Ag/AgCl reference electrode. In the anodic sweep, iodide is oxidized to triiodide according to reaction (5), and when the potential scan is reversed, triiodide is reduced to iodide [38]:

$$3I^- \rightleftarrows I_3^- + 2e^- \quad (5)$$

Fig. 7 reveals that the cathodic peak shifts more negatively and the anodic peak shifts more positively in the presence of amylopectin compared to those in the absence of amylopectin. Because the magnitudes of the shifts are approximately equal, the reduction potential of the I_3^-/I^- couple appears not to be influenced by the formation of the amylopectin–I_2 complex. The formation of the amylopectin–I_2 complex apparently does not change the V_{red} value of I_3^-/I^- redox couple in DMSO. Therefore, it is concluded that the decrease in the V_{oc} value in Fig. 2 is predominantly due to the increased back electron transfer arising from the increased concentration of I_3^- in the TiO_2 film.

3.5. Corrosion of silver metal

Fig. 8 reveals that the potentiodynamic polarization curves for silver metal by the I_3^-containing electrolyte in DMSO. The corresponding inhibition efficiency (IE) was calculated using the equation:

$$IE(\%) = \frac{i^0 - i}{i^0} \times 100 \quad (6)$$

where i^0 and i are the corrosion current measured in the absence and presence of amylopectin, respectively. The enhanced corrosion efficiency in the presence of amylopectin shown in Table 4 is attributable to the decreased contact of silver metal with iodine as a result of the formation of amylopectin–I_2 complex. This result suggests that the dissolution of silver grids by iodine, $2Ag(s) + I_3^- \leftrightarrows 2Ag^+ + 3I^-$, in the DSSC modules of commercial uses can be protected by formation of the complexes of iodine with suitable complex-forming agents.

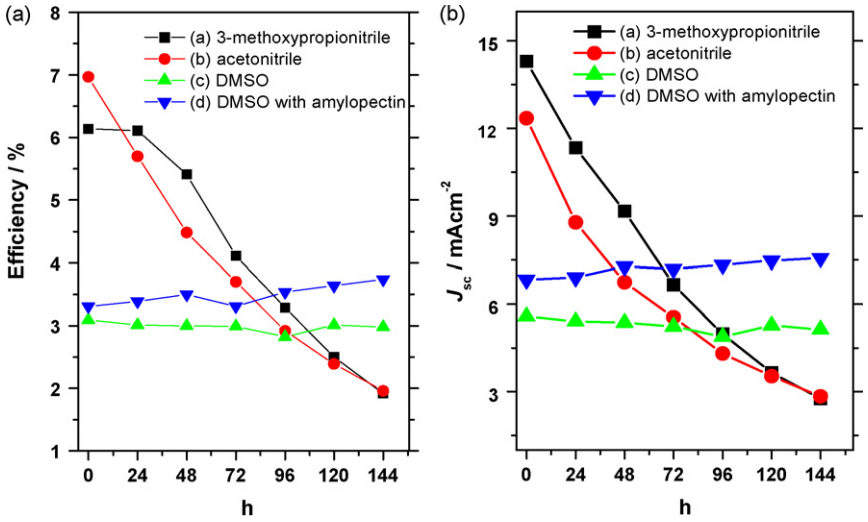

Fig. 9. Solvent dependence of (a) solar-to-electricity conversion efficiency (η) and (b) short-circuit current density (J_{sc}) of the DSSC as a function of time.

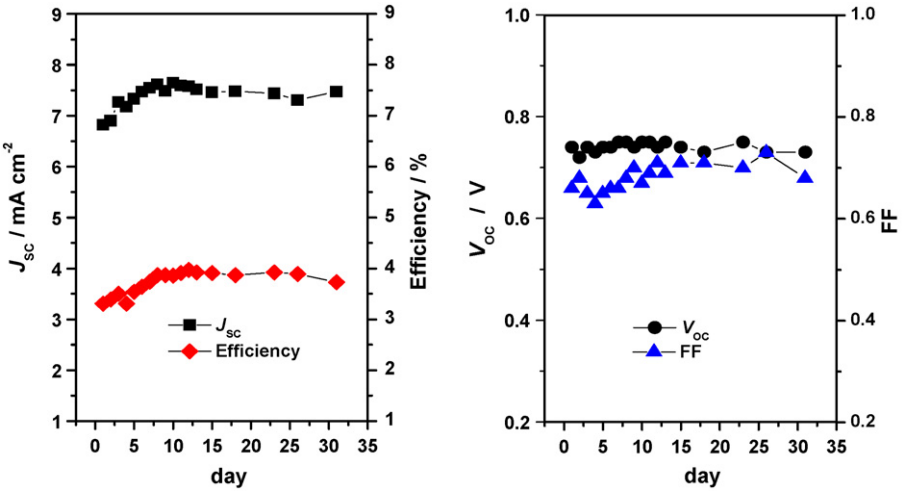

Fig. 10. Variation of photovoltaic parameters of a DSSC assembled with the electrolyte containing 1.5×10^{-2} M of amylopectin in DMSO over a period of 31 d.

Table 4
Potentiodynamic polarization parameters of the DSSCs fabricated using different concentrations of amylopectin[a].

Amylopectin (M)	Current (mA)	IE (%)
0.0	2.69	–
2.2×10^{-3}	0.51	81
8.7×10^{-3}	0.48	82
1.5×10^{-2}	0.30	89
2.2×10^{-2}	0.21	92

[a] The same electrolyte as in Table 1.

3.6. Long-term stability

For comparison of the stability of the DSSC, three reference solar cells without amylopectin in commonly used 3-methoxypropionitrile and acetonitrile solvents in addition to DMSO were assembled according to the method described in Section 2. The cells were stored in a desiccator and subjected to electrochemical measurements every 24 h at room temperature. The variations of the efficiency and J_{sc} of these four cells are compared in Fig. 9a and b, respectively, over 6 d. The efficiencies of the solar cells with the liquid electrolyte in 3-methoxypropionitrile and acetonitrile without amylopectin decrease dramatically with time, due to the leakage of the organic solvents through the polyimide film. The viscosities at 25 °C are 0.375 mP s, 1.1 mP s and 1.996 mP s for acetonitrile, 3-methoxypropionitrile and DMSO, respectively [39]. On the other hand the efficiency of the electrolyte with amylopectin increased by 13% from its initial value. Finally, Fig. 10 shows the photovoltaic characteristics of the DSSCs based on the electrolyte containing amylopectin in DMSO. It is noted that the V_{oc} value of the DSSC did not vary much over a period of 31 d. The J_{sc}, FF and η values of the DSSC increased slightly over the same period.

4. Conclusions

A comparative study on the photoelectrochemical characteristics of DSSCs was carried out in highly viscous DMSO solutions with and without amylopectin. The DSSCs with the electrolyte containing amylopectin rendered a solar-to-electricity conversion efficiency of 3.34%, compared to 3.08% for the reference cell prepared without amylopectin primarily due to the enhanced photocurrent. The improved stability of the DSSC with amylopectin is attributed to the increased viscosity of the electrolytic solution when compared with the reference cell. The electrolyte with amylopectin was found to be corrosion resistant for silver metal. It is therefore expected that electrolytes containing amylopectin would be an attractive alternative to conventional liquid electrolytes for the fabrication of DSSCs with long-term stability that are free from the problems of solvent evaporation and leakage. It would be highly beneficial for the increased efficiency of DSSCs if amylopectin could be functionalized to enhance its solubility in less viscous common solvents such as 3-methoxypropionitrile or acetonitrile than DMSO.

Acknowledgment

This work was supported by the MKE new and renewable energy R&D project under contract 2006-N-PV12-P-05.

References

[1] J.H. Wu, S.C. Hao, Z. Lan, J.M. Lin, M.L. Huang, Y.F.L. Huang, Q. Fang, S. Yin, T. Sato, A thermoplastic gel electrolyte for stable quasi-solid-state dye-sensitized solar cells, Adv. Funct. Mater. 17 (2007) 2645–2652.
[2] P.G. Bruce (Ed.), Solid-state Electrochemistry, Cambridge University Press, Cambridge, 1995.
[3] F.M. Gray, Polymer Electrolytes, The Royal Society of Chemistry Materials Monographs, Cambridge, 1997.
[4] W.H. Meyer, Polymer electrolytes for lithium-ion batteries, Adv. Mater. 10 (1998) 439–448.
[5] C. Scoenenberger, J.-F. Le Nest, A. Gandini, Polymer electrolytes based on modified polysaccharides. 2. Polyether-modified cellulosics, Electrochim. Acta 40 (1995) 2281–2284.
[6] P.V. Morales, J.-F. Le Nest, A. Gandini, Polymer electrolytes derived from chitosan/polyether networks, Electrochim. Acta 43 (1998) 1275–1279.
[7] A.M. Regiani, C.E. Tambelli, A. Pawlicka, A.A.S. Curvelo, A. Gandini, J.-F. Le Nest, J.P. Donoso, DSC and solid state NMR characterization of hydroxyethylcellulose/polyether films, Polym. Int. 49 (2000) 960–964.
[8] C.E. Tambelli, J.P. Donoso, A.M. Regiani, A. Pawlicka, A. Gandini, J.-F. Le Nest, Nuclear magnetic resonance and conductivity study of HEC/polyether-based polymer electrolytes, Electrochim. Acta 46 (2001) 1665–1672.
[9] D.C. Dragunski, A. Pawlicka, Starch based solid polymeric electrolytes, Mol. Cryst. Liquid Cryst. 374 (2002) 561–568.
[10] H. Davis, W. Skrzypek, A. Khan, Iodine binding by amylopectin and stability of the amylopectin–iodine complex, J. Polym. Sci. Part A: Polym. Chem. 32 (1994) 2267–2274.
[11] M. Grätzel, Conversion of sunlight to electric power by nanocrystalline dye-sensitized solar cells, J. Photochem. Photobiol. A: Chem. 164 (2004) 3–14.
[12] Y. Chiba, A. Islam, Y. Watanabe, R. Komiya, N. Koide, L. Han, Dye-sensitized solar cells with conversion efficiency of 11.1%, Jpn. J. Appl. Phys. 45 (2006) L638–L640.
[13] S. Murai, S. Mikoshiba, H. Sumino, T. Kato, S. Hayase, Quasi-solid dye sensitized solar cells filled with phase-separated chemically cross-linked ionic gels, Chem. Commun. (2003) 1534–1535.
[14] B. O'Regan, D.T. Schwartz, Large enhancement in photocurrent efficiency caused by UV illumination of the dye-sensitized heterojunction TiO_2/RuLL'NCS/CuSCN: initiation and potential mechanisms, Chem. Mater. 10 (1998) 1501–1502.

[15] B. O'Regan, F. Lenzmann, R. Muis, J. Wienke, A solid-state dye-sensitized solar cell fabricated with pressure-treated P25–TiO_2 and CuSCN: analysis of pore filling and IV characteristics, Chem. Mater. 14 (2002) 5023–5029.
[16] U. Bach, D. Lupo, P. Comte, M. Grätzel, Solid-state dye-sensitized mesoporous TiO_2 solar cells with high photon-to-electron conversion efficiencies, Nature 395 (1998) 583–585.
[17] R. Senadeera, N. Fukuri, Y. Satio, Volatile solvent-free solid-state polymer-sensitized TiO_2 solar cells with poly(3, 4-ethylenedioxythiophene) as a hole-transporting medium, Chem. Commun. (2005) 2259–2261.
[18] S. Spiekermann, G. Smestad, J. Kowalik, M. Grätzel, Poly(4-undecyl-2,2′-bithiophene) as a hole conductor in solid state dye sensitized titanium dioxide solar cells, Synth. Met. 121 (2001) 1603–1604.
[19] H. Usui, H. Mataui, N. Tanabe, S. Yanagida, Improved dye-sensitized solar cells using ionic nanocomposite gel electrolytes, J. Photochem. Photobiol. A: Chem. 164 (2004) 97–101.
[20] J. Xia, F. Li, C.H. Huang, Improved stability quasi-solid-state dye-sensitized solar cell based on polyether framework gel electrolytes, Sol. Energy Mater. Sol. Cells 90 (2006) 944–952.
[21] P. Wang, S.M. Zakeeruddin, J.E. Moser, M. Grätzel, A stable quasi-solid-state dye-sensitized solar cell with an amphiphilic ruthenium sensitizer and polymer gel electrolyte, Nat. Mater. 2 (2003) 402–407.
[22] F. Cao, G. Oskam, P.C. Searson, Solid state dye sensitized photoelectrochemical cell, J. Phys. Chem. 99 (1995) 17071–17073.
[23] J. Wu, Z. Lan, D. Wang, S. Hao, J. Lin, Y. Wei, Y. Shu, T. Sato, Quasi-solid state dye-sensitized solar cells-based gel polymer electrolytes with poly(acrylamide)–poly(ethylene glycol) composite, J. Photochem. Photobiol. A: Chem. 181 (2006) 333–337.
[24] Z. Lan, J.H. Wu, D.B. Wang, S.C.J.M. Lin, Quasi-solid state dye-sensitized solar cells based on gel polymer electrolyte with poly(acrylonitrile-co-styrene)/NaI + I_2, Sol. Energy 80 (2006) 1483–1488.
[25] W. Kubo, S. Kambe, S. Nakade, T. Kitamura, K. Hanabusa, Y. Wada, Photocurrent-determining processes in quasi-solid-state dye-sensitized solar cells using ionic gel electrolytes, J. Phys. Chem. B 107 (2003) 4374–4381.
[26] T. Kato, A. Okazaki, S. Hayase, Latent gel electrolyte precursors for quasi-solid dye sensitized solar cells: the comparison of nano-particle cross-linkers with polymer cross-linkers, J. Photochem. Photobiol. A: Chem. 179 (2006) 42–48.
[27] W. Li, J. Kang, X. Li, S. Fang, Y. Lin, G. Wang, X. Xiao, A novel polymer quaternary ammonium iodide and application in quasi-solid-state dye-sensitized solar cells, J. Photochem. Photobiol. A: Chem. 170 (2005) 1–6.
[28] W.J. Lee, E. Ramasamy, D.Y. Lee, J.S. Song, Grid type dye-sensitized solar cell module with carbon counter electrode, J. Photochem. Photobiol. A: Chem. 194 (2008) 27–30.
[29] M.G. Kang, N.-G. Park, S.H. Chang, S.H. Choi, K.-J. Kim, Enhanced photocurrent of Ru(II)-dye sensitized solar cells by incorporation of titanium silicalite-2 in TiO_2 film, Bull. Kor. Chem. Soc. 23 (2002) 140–142.
[30] A. Fukui, R. Komiya, R. Yamanaka, A. Islam, L. Han, Effect of a redox electrolyte in mixed solvents on the photovoltaic performance of a dye-sensitized solar cell, Sol. Energy Mater. Sol. Cells 90 (2006) 649–658.
[31] V. Suryanarayanan, K.-M. Lee, J.-G. Chen, K.-C. Ho, High performance dye-sensitized solar cells containing 1-methyl-3-propyl imidazolinium iodide—effect of additives and solvents, J. Electroanal. Chem. (2009) 005, 1016/j.jelectrochem.2009.05.
[32] F. Fabregat-Santiago, J. Bisquert, E. Palomares, L. Otero, D. Kuang, S.M. Zakeeruddin, M. Grätzel, Correlation between photovoltaic performance and impedance spectroscopy of dye sensitized solar cells based on ionic liquids, J. Phys. Chem. C 111 (2007) 6550–6560.
[33] Y.V. Pleskov, Y.Y. Gurevich, Semiconductor Photoelectrochemistry, Consultants Bureau, New York, 1986, p. 120.
[34] S. Uchida, M. Tomiha, Y. Sanehira, Y. Fushimi, Solar cells dye-sensitized with β-CDI in electrolyte, Jpn. J. Polym. Sci. Technol. 63 (2006) 62–67.
[35] Z. Kebede, S.E. Lindquist, Donor–acceptor interaction between non-aqueous solvents and I_2 to generate I_3^-, and its implication in dye sensitized solar cells, Sol. Energy Mater. Sol. Cells 57 (1999) 259–275.
[36] Y.V. Pleskov, Y.Y. Gurevich, Semiconductor Photoelectrochemistry, Consultants Bureau, New York, 1986, p. 241.
[37] H.O. Finklea, Semiconductor Electrodes, Elsevier, New York, 1988, p. 31.
[38] K.J. Hansen, C.W. Tobias, Electrochemistry of iodide in propylene carbonate, J. Electrochem. Soc. 134 (1987) 2204–2210.
[39] J.A. Riddick, W.B. Bunger (Eds.), Organic Solvents—Physical Properties and Methods of Purification, Techniques of Chemistry, vol. II, Wiley-Interscience, New York, 1970.